ChemComm

COMMUNICATION

View Article Online
View Journal | View Issue

Cite this: *Chem. Commun.*, 2022, **58**, 10805

Received 28th April 2022,
Accepted 5th August 2022

DOI: 10.1039/d2cc02402k

rsc.li/chemcomm

Atmospheric pressure atomic layer deposition to increase organic solvent resistance of PDMS†

Albert Santoso, Afke Damen, J. Ruud van Ommen and Volkert van Steijn *

We explore three variants of atomic layer deposition (ALD) to deposit titanium oxide on the soft polymer polydimethylsiloxane (PDMS). We show that the organic solvent resistance of PDMS is increased by two orders of magnitude compared to uncoated PDMS for ALD performed at atmospheric pressure, which results in a unique surface–subsurface coating of PDMS.

Since its introduction as a material for microfluidics in 1998,[1] the rise of polydimethylsiloxane (PDMS) has revolutionized research in medicine, biology, and chemistry.[2] While PDMS is easy to micromold, cheap, and amicable in rapid prototyping, it has one major drawback: its poor chemical resistance against common organic solvents.[1–5] Upon contact, PDMS swells and deforms, rendering it useless in many applications such as solvent-based extraction, production of liposomes, and flow chemistry for organic synthesis. Currently, most approaches focus on the use of inert coatings such as glass-like materials and fluoro-based polymers.[6–9] The coating processes, however, involve difficult, costly or time-consuming steps.[10–12] Furthermore, the resulting coatings are typically relatively thick with respect to the features of the microchannels, such that the properties of the channel walls do not stem from the soft and pliant bulk properties of PDMS, but from the hard and brittle surface properties of the coating.[7]

To overcome inherent disadvantages of existing PDMS coatings, metal oxide nano-films present a promising class of materials due to their ability to withstand organic solvents[13,14] while being nanoscopically thin and faithfully following the structures of the PDMS. Among many surface deposition techniques, atomic layer deposition (ALD) stands out for its high uniformity, even when coating complex structures.[15] This uniformity stems from the successive build up of the coating by exposing a surface to alternating, self-limiting reactions.[15] It is hence interesting to explore the coating of PDMS with metal oxide nano-films through ALD in order to achieve organic solvent resistance of PDMS.

A general challenge in coating polymers with a thin layer of metal oxide through ALD arises from the difference in thermal expansion coefficient of the metal oxide coating and the polymer. Thermal expansion or contraction leads to cracks in the coating,[16–20] compromising its performance.[16–23] Adding intermediate layers may solve this problem, at the expense of a more complex process.[20] While there is significant advancement on ALD coating of hard-set polymers such as polyethylene, polypropylene, polyethylene terephthalate, and polylactic acid,[24–26] examples of successful ALD coatings on PDMS are scarce. The additional complexity arises from the non-reactive porous nature of PDMS,[16] such that the reactions are not only confined to the surface, but also take place in the subsurface of the PDMS. This turns ALD coating of PDMS into a complex reaction–diffusion problem, in which reactivity, reactant residence time, operating conditions and substrate pre-treatment all play a role in the resulting morphology.[27–30] Even when moderate temperature, time-consuming steps or rigorous sample preparations are employed, studies so far reported metal oxide layers on PDMS with varying degree of conformality and robustness.[16,28,29] An outstanding challenge hence is the development of a simple ALD process for metal oxides on PDMS to significantly expand the use of PDMS in practical applications involving the use of organic solvents.

In this paper, we explore three variants of ALD to coat titanium oxide on PDMS. Aside from its resistance against organic solvents, titanium oxide is chosen over other metal oxides for its relatively mild ALD precursors.[13,14] We show that the three variants lead to three different types of treatments: a surface treatment, a subsurface treatment, and a combined surface–subsurface treatment. We tested the resistance of the resulting coatings against a variety of common solvents and found the surface–subsurface treatment to be the most successful, with an increase in chemical resistance over two orders of magnitude as compared to untreated PDMS.

We fabricated PDMS samples by mixing Sylgard 184 elastomer (Dow-Corning) and its curing agent in a 10 to 1 weight ratio and subsequent curing of the mixture at 200 °C for at least

Department of Chemical Engineering, Delft University of Technology, Delft, The Netherlands. E-mail: v.vansteijn@tudelft.nl

† Electronic supplementary information (ESI) available. See DOI: https://doi.org/10.1039/d2cc02402k

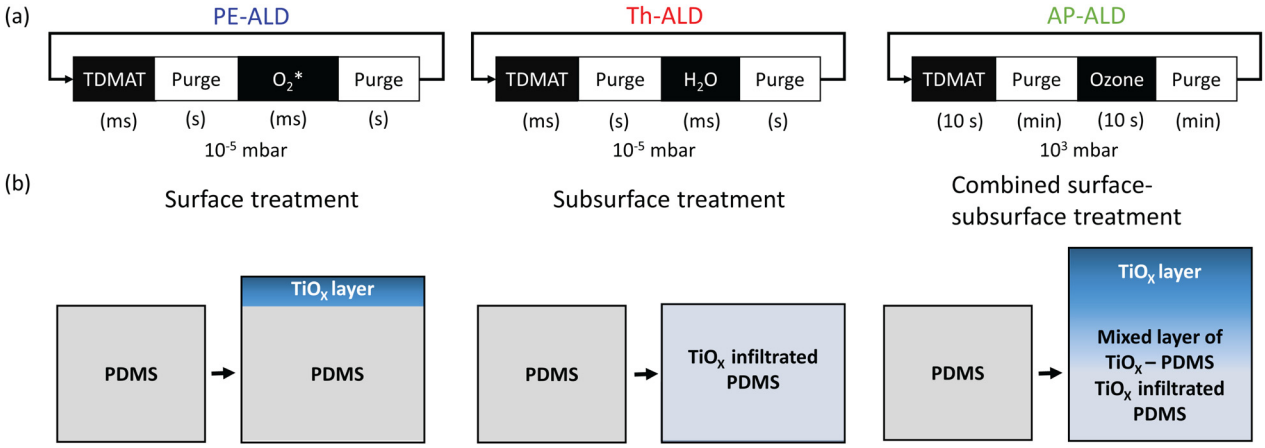

Fig. 1 (a) Illustration of three different variants of ALD and (b) simplified representations of the resulting deposition profiles (details in Fig. 2).

10 hours. PDMS samples were treated with ALD using a Ti precursor (tetrakis(dimethylamino)titanium, TDMAT) and an oxidizing agent. Reactants were sequentially introduced into the ALD reactor chamber. In between, the reactor was purged with an inert gas. Unless stated otherwise, we repeated this sequence, known as an ALD cycle, 100 times and carried out the ALD process at 100 °C. The difference between the three explored ALD variants stems from the used oxidizing agent, the used pressure, and the used reactant pulse and purge times, see Fig. 1a. We used a strong and a mild oxidizing agent. As demonstrated later, the former led to a nanoscopically thin TiO_x coating on the PDMS surface, while the latter led to infiltration of TiO_x inside the PDMS, see the left and middle panel in Fig. 1b. As strong oxidizing agent, we used oxygen plasma and refer to this first variant as plasma enhanced ALD (PE-ALD). As mild oxidizing agent, we used water vapour and refer to this second variant as thermal ALD (Th-ALD). Besides these two variants carried out at vacuum, we also performed ALD at atmospheric pressure, requiring comparatively longer times for the pulse and purge steps. As demonstrated later, this led to a combined surface–subsurface layer of TiO_x, see the right panel in Fig. 1b. Here, we used ozone as the oxidizing agent and refer this third variant as atmospheric pressure ALD (AP-ALD). Further details are given in Section S1 in the ESI.†

We analysed the surface and subsurface of the ALD coated PDMS samples using X-ray photoelectron spectroscopy (XPS). To obtain the elemental analysis of the surface and subsurface, we sequentially etched the surface for 5–50 seconds with an ion-beam etching unit and then performed an XPS reading. To convert the etch time into an etch depth, we placed a silicon wafer next to the PDMS samples during the ALD process, to coat them with TiO_x, and subsequently performed comparative etching measurements, see Section S1 and Fig. S7 (ESI†) for details. We note that ALD on soft materials such as PDMS where infiltration may occur is more ambiguous to characterize than ALD on hard materials without infiltration. We therefore choose to omit the commonly used concept of growth per cycle.

Fig. 2a shows how the atomic percentage of titanium changes along the depth of the PDMS samples coated with

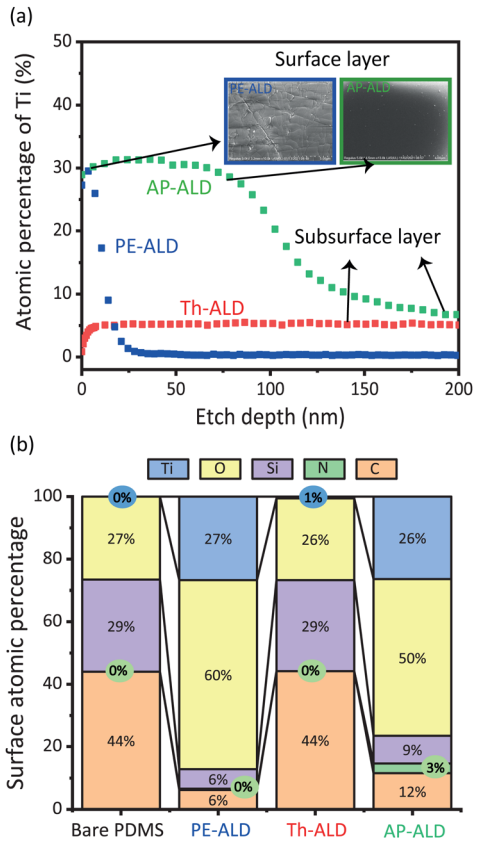

Fig. 2 (a) XPS depth profiling showing the atomic percentage of titanium in the surface and subsurface of various PDMS samples and (b) XPS elemental analysis of the surface. All depositions were conducted at 100 °C for 100 cycles, and the TiO_x layer thickness is estimated to be 7 and 78 nm for the PE-ALD and AP-ALD treated samples, respectively.

the three ALD variants. The PE-ALD treated PDMS shows a significant atomic percentage of titanium at the surface (before etching). After 7 nm, the percentage rapidly drops to zero. A closer look at the XPS surface spectra confirms the dominance of titanium and oxygen atoms, with an atomic ratio of about 1 to 2, indicating TiO_2 deposition on the surface (Fig. 2b). PE-ALD

hence leads to a layer of TiO_x at the surface of the PDMS. In sharp contrast, PDMS treated with Th-ALD shows hardly any titanium on the surface itself (Fig. 2a). In fact, the surface composition is comparable to bare PDMS, as evident from Fig. 2b. Interestingly, a meaningful percentage of titanium ($\sim$5%) is found in the subsurface of the PDMS, over an etch depth of $\sim$200 nm, see Fig. 2a. Th-ALD hence leads to a TiO_x infiltrated PDMS layer. From the above findings, we infer that the high reactivity of the oxygen plasma leads to nucleation only at the surface of the PDMS, while the lower reactivity of water vapour allows for the diffusion of both reactants into the PDMS pores, in line with earlier work.[16,27–29]

Unique to this work is AP-ALD coating of PDMS. Elemental analysis shows an atomic percentage of titanium at the surface comparable to PE-ALD, indicating the presence of a surface layer. Strikingly different from PE-ALD, the atomic percentage decreases more gradual with etch depth and does not drop to zero over a depth of $\sim$5200 nm, but approaches the value for Th-ALD. While a higher TiO_x loading of AP-ALD with respect to the two vacuum-based variants (PE-ALD and Th-ALD) is understood from higher partial pressures of the reactants, the formation of a surface-subsurface layer is understood from the balance between the reactivity of the ozone as oxidizing agent on the one hand, and the diffusion properties of the reactants on the other hand, allowing for simultaneous infiltration and surface reaction. AP-ALD treatment of PDMS hence results in a unique surface–subsurface coating. We note that an additional XPS test shows that the ratio of Ti:O on the surface remains the same with 20 and 250 cycles for all three ALD variants.

With three distinctly different TiO_x coatings on PDMS obtained, we now continue testing the coatings for their resistance against organic solvents. Organic resistance of ALD coated and bare PDMS was tested by immersing the samples in a beaker with organic solvent for a given exposure time and measuring the mass of the samples before and after immersion, as illustrated in Fig. 3a. To remove solvent adhering to the samples, samples were briefly blown dry using compressed nitrogen. As a model organic solvent, we used cyclohexane (Sigma-Aldrich). As well known, the uptake of cyclohexane by bare PDMS is significant.[4] This is confirmed in our experiments, see the increase in mass relative to the initial mass plotted in Fig. 3b. Th-ALD treated PDMS, with an infiltrated TiO_x subsurface, but no TiO_x surface, shows a similar trend. The slightly reduced uptake indicates that the TiO_x infiltrated subsurface layer has potential to decrease the organic solvent uptake, yet to a small extent. PE-ALD treated PDMS, with a TiO_x surface, but no TiO_x subsurface, shows a much stronger reduction in uptake. AP-ALD treated PDMS, with a TiO_x surface as well as a TiO_x subsurface, shows virtually no uptake, with a fractional mass increase of 0.0035 g g^{-1} after 24 h of immersion. Even after 240 h, there is only a slight increase, hence the coating is considered durable. Compared to 0.15 g g^{-1} for bare PDMS after 24 h, the reduction in uptake is two orders of magnitude for AP-ALD treated PDMS. To test whether it is the thickness of the surface layer or the presence of a subsurface

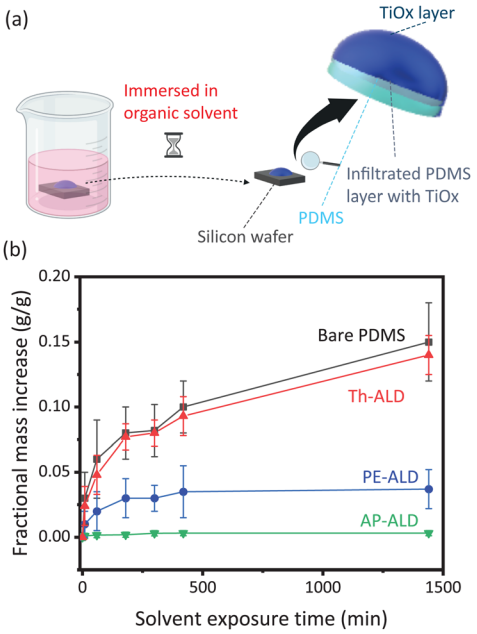

Fig. 3 (a) Measurement of organic solvent resistance performance of the samples (made with biorender.com), (b) fractional mass increase of bare and ALD-treated PDMS, cured at 200 °C. Error bars of bare PDMS were calculated as the standard deviation of 20 samples per time point, while error bars of the ALD treated PDMS were based on 3 samples.

layer that explains the reduced uptake for AP-ALD treated PDMS (0.0035 g g^{-1} after 24 h) in reference to PE-ALD treated PDMS (0.037 g g^{-1} after 24 h), we performed additional PE-ALD experiments by using 20, 300 and 700 ALD cycles. While the resulting TiO_x surface layer was 1 nm, 22 nm and 54 nm respectively, we did not observe significant reduction of the uptake after 24 h (0.14, 0.035 and 0.034 g g^{-1}). Additionally, we performed an AP-ALD experiment with 50 cycles and found a fractional mass increase of 0.0031 g g^{-1} after 24 h of immersion. These experiments indicate that the organic solvent resistance is not attributed to the surface layer thickness, but to the combined surface–subsurface structure. To gain further insight, we pretreated a PDMS sample with oxygen plasma before treating it with Th-ALD; we also pretreated a PDMS sample with Th-ALD before treating it with PE-ALD. On both samples, we observed the organic resistance performance was comparable with PE-ALD treated samples, due to absence of a unique surface–subsurface layer. This further supports the finding that atmospheric pressure is key.

Before examining the ALD coated samples in more detail, we point out the importance of the temperature used to cure PDMS. Fig. S1 (ESI†) is equivalent to Fig. 3, but for a curing temperature of 70 °C instead of 200 °C. Rather than a monotonic increase in uptake over time, all curves show a rapid initial uptake, to much higher values than for 200 °C, followed by a decrease. This decrease is explained by leaching of monomers from the PDMS, a well reported phenomena.[31] The mass and internal structure of PDMS hence changes during immersion. For bare and Th-ALD treated PDMS, with no or little TiO_x

barrier, the final value (after 24 h) is comparable to PDMS cured at 200 °C. However, for PE-ALD and AP-ALD treated samples, with a significant TiO_x barrier, restructuring of the PDMS due to leaching compromises the barrier, such that the final values (after 24 h) are significantly larger for PDMS cured at 70 °C than at 200 °C. These comparative experiments illustrate the importance to cure the PDMS at a sufficiently high temperature to minimize leaching of monomers, because leaching compromises the surface and subsurface coating due to restructuring of PDMS upon contact with organic solvents. Besides cyclohexane as model solvent, we also tested the resistance of AP-ALD coated PDMS for other common solvents. These experiments show a comparable resistance, see Fig. S2 (ESI†). While a TiO_x layer is relatively stable against various organic solvents and alkaline solution, it should be noted that it dissolves in acids such as 0.1 M HNO_3. For applications involving acids, other metal oxides should be considered such as SiO_x.

To investigate why AP-ALD samples performed better than the PE-ALD ones, we examined the surface morphology using field emission scanning electron microscopy (FE-SEM, Hitachi Regulus SU8230). While all samples appear visually transparent and are comparable with bare PDMS (Fig. S6, ESI†), Fig. S3 (ESI†) shows visible cracks on the PE-ALD samples, and not on the AP-ALD samples. While no cracks are visible on the Th-ALD samples, the SEM images confirm that there is virtually no TiO_x layer present, explaining its poor solvent resistance. To approximate the crack depth of the PE-ALD samples, we conducted atomic force microscopy. The average crack depth is up to 100 nm (Fig. S5, ESI†). With an estimated TiO_x layer thickness of 7 nm on PE-ALD surfaces, cracks hence extend deep into the PDMS layer, allowing direct contact between organic solvent and PDMS. Whether cracks were formed during the ALD process due to thermal expansion of PDMS[18] or afterwards due to a difference between strains on sharply divided layers[32] remains a question, which is beyond the scope of this study. Cracks were not observed in the AP-ALD samples. We hence expect that the unique and gradual surface–subsurface layer formed by AP-ALD (Fig. 2a) prevents crack formation due to thermal expansion and undistributed residual strain loads, explaining limited swelling upon contact with organic solvents. In follow-up experiments, we explored the effect of the operating parameters of AP-ALD on the solvent resistance, highlighting a lower limit for the number of cycles and an upper limit for the deposition temperature (Fig. S4, ESI†).

In conclusion, we found that the deposition of TiO_x on the soft polymer PDMS using AP-ALD results in a combined surface–subsurface coating. We demonstrated that this coating acts as a barrier against organic solvents, limiting the issue of swelling that is often a challenge in the application of PDMS. By using simpler atmospheric operation instead of vacuum technologies, this proof-of-principle brings the application of ALD on polymers closer to commercial realizations.

This publication is part of the Open Technology programme financed by the Dutch Research Council (NWO). We thank Mojgan Talebi and Bart Boshuizen for their technical support.

Conflicts of interest

There are no conflicts to declare.

References

1 J. C. McDonald, D. C. Duffy, J. R. Anderson, D. T. Chiu, H. Wu, O. J. Schueller and G. M. Whitesides, *Electrophoresis*, 2000, **21**, 27–40.
2 K. Raj M and S. Chakraborty, *J. Appl. Polym. Sci.*, 2020, **137**, 48958.
3 Y. Hwang and R. N. Candler, *Lab Chip*, 2017, **17**, 3948–3959.
4 J. N. Lee, C. Park and G. M. Whitesides, *Anal. Chem.*, 2003, **75**, 6544–6554.
5 R. Dangla, F. Gallaire and C. N. Baroud, *Lab Chip*, 2010, **10**, 2972–2978.
6 B.-Y. Kim, L.-Y. Hong, Y.-M. Chung, D.-P. Kim and C.-S. Lee, *Adv. Funct. Mater.*, 2009, **19**, 3796–3803.
7 A. R. Abate, D. Lee, T. Do, C. Holtze and D. A. Weitz, *Lab Chip*, 2008, **8**, 516–518.
8 T. J. Renckens, D. Janeliunas, H. van Vliet, J. H. van Esch, G. Mul and M. T. Kreutzer, *Lab Chip*, 2011, **11**, 2035–2038.
9 T. Yang, J. Choo, S. Stavrakis and A. de Mello, *Chem. – Eur. J.*, 2018, **24**, 12078–12083.
10 S. Goyal, A. V. Desai, R. W. Lewis, D. R. Ranganathan, H. Li, D. Zeng, D. E. Reichert and P. J. Kenis, *Sens. Actuators, B*, 2014, **190**, 634–644.
11 A. Vitale, M. Quaglio, S. L. Marasso, A. Chiodoni, M. Cocuzza and R. Bongiovanni, *Langmuir*, 2013, **29**, 15711–15718.
12 F. Kotz, P. Risch, D. Helmer and B. E. Rapp, *Micromachines*, 2018, **9**, 115.
13 J. P. Niemelä, G. Marin and M. Karppinen, *Semicond. Sci. Technol.*, 2017, **32**, 093005.
14 K. Liu, M. Cao, A. Fujishima and L. Jiang, *Chem. Rev.*, 2014, **114**, 10044–10094.
15 H. Van Bui, F. Grillo and J. R. van Ommen, *Chem. Commun.*, 2017, **53**, 45–71.
16 J. C. Spagnola, B. Gong and G. N. Parsons, *J. Vac. Sci. Technol., A*, 2010, **28**, 1330–1337.
17 H. C. Guo, E. Ye, Z. Li, M.-Y. Han and X. J. Loh, *Mater. Sci. Eng. Carbon*, 2017, **70**, 1182–1191.
18 G. N. Parsons, S. E. Atanasov, E. C. Dandley, C. K. Devine, B. Gong, J. S. Jur, K. Lee, C. J. Oldham, Q. Peng and J. C. Spagnola, *et al.*, *Coord. Chem. Rev.*, 2013, **257**, 3323–3331.
19 A. Bulusu, S. Graham, H. Bahre, H. Behm, M. Böke, R. Dahlmann, C. Hopmann and J. Winter, *Adv. Eng. Mater.*, 2015, **17**, 1057–1067.
20 A. Behrendt, J. Meyer, P. van de Weijer, T. Gahlmann, R. Heiderhoff and T. Riedl, *ACS Appl. Mater. Interfaces*, 2016, **8**, 4056–4061.
21 K. L. Jarvis and P. J. Evans, *Thin Solid Films*, 2017, **624**, 111–135.
22 S.-H. Jen, J. A. Bertrand and S. M. George, *J. Appl. Phys.*, 2011, **109**, 084305.
23 F. Nehm, H. Klumbies, C. Richter, A. Singh, U. Schroeder, T. Mikolajick, T. Monch, C. Hoßbach, M. Albert and J. W. Bartha, *et al.*, *ACS Appl. Mater. Interfaces*, 2015, **7**, 22121–22127.
24 J. H. Jang, N. Kim, X. Li, T. K. An, J. Kim and S. H. Kim, *Appl. Surf. Sci.*, 2019, **475**, 926–933.
25 T. O. Kääriäinen, P. Maydannik, D. C. Cameron, K. Lahtinen, P. Johansson and J. Kuusipalo, *Thin Solid Films*, 2011, **519**, 3146–3154.
26 K. Lahtinen, P. Maydannik, P. Johansson, T. Kääriäinen, D. C. Cameron and J. Kuusipalo, *Surf. Coat. Technol.*, 2011, **205**, 3916–3922.
27 E. Y. Choi, J.-H. Kim, B.-J. Kim, J. H. Jang, J. Kim and N. Park, *RSC Adv.*, 2019, **9**, 11737–11744.
28 S. H. Astaneh, G. Jursich, C. Sukotjo and C. G. Takoudis, *Appl. Surf. Sci.*, 2019, **493**, 779–786.
29 B. Gong, J. C. Spagnola and G. N. Parsons, *J. Vac. Sci. Technol., A*, 2012, **30**, 01A156.
30 S.-M. Lee, E. Pippel, U. Gösele, C. Dresbach, Y. Qin, C. V. Chandran, T. Bräuniger, G. Hause and M. Knez, *Science*, 2009, **324**, 488–492.
31 K. J. Regehr, M. Domenech, J. T. Koepsel, K. C. Carver, S. J. Ellison-Zelski, W. L. Murphy, L. A. Schuler, E. T. Alarid and D. J. Beebe, *Lab Chip*, 2009, **9**, 2132–2139.
32 Y. Li, Y. Xiong, H. Yang, K. Cao and R. Chen, *J. Mater. Res.*, 2020, **35**, 681–700.

